Chapter 12

Optically Induced Damage and Multiphoton Absorption

12.1 Introduction to Optical Damage

A topic of great practical importance is optically induced damage of optical components. Optical damage is important because it ultimately limits the maximum amount of power that can be transmitted through a particular optical material. Optical damage thus imposes a constraint on the efficiency of many nonlinear optical processes in that it limits the maximum field strength E that can be used to excite the nonlinear response. In this context, it is worth pointing out that present laser technology can produce laser beams of sufficient intensity to exceed the damage thresholds of all known materials. Additional information regarding the properties of laser-induced material damage can be found in Bloembergen (1974), Lowdermilk and Milam (1981), Manenkov and Prokhorov (1986), Raizer (1965), and Wood (1986).

There are several different physical mechanisms that can lead to optically induced damage. These mechanisms, and an approximate statement of the conditions under which each might be observed, are as follows:

- Linear absorption, leading to localized heating and cracking of the optical material. This is the dominant damage mechanism for continuous-wave and long-pulse ($\gtrsim 1$ μsec) laser beams.
- Avalanche breakdown, which is the dominant mechanism for pulsed lasers (shorter than $\lesssim$1 μsec) for intensities in the range of 10^9 W/cm^2 to 10^{12} W/cm^2.
- Multiphoton ionization or multiphoton dissociation of the optical material, which is the dominant mechanism for intensities in the range 10^{12} to 10^{16} W/cm^2.
- Direct (single cycle) field ionization, which is the dominant mechanism for intensities $>10^{20}$ W/cm^2.

We begin by briefly summarizing some of the basic empirical observations regarding optical damage. When a collimated laser beam interacts with an optical material, optical damage

Nonlinear Optics. https://doi.org/10.1016/B978-0-12-811002-7.00021-7

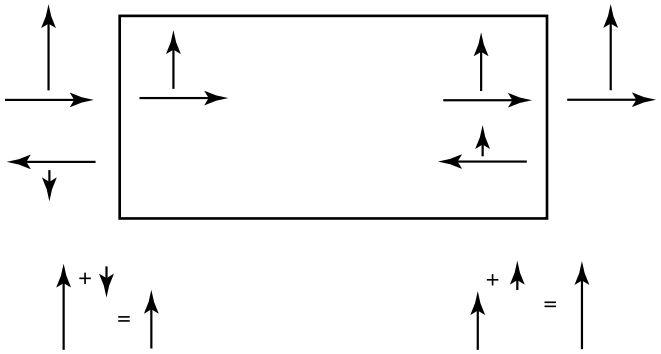

FIGURE 12.1.1: For a collimated laser beam, optical damage tends to occur at the exiting surface of an optical material, because the boundary conditions on the electric field vector lead to an enhancement at the exiting surface and a deenhancement at the entering surface.

usually occurs at a lower threshold on the surfaces than in the interior. This observation suggests that cracks and other imperfections on an optical surface can serve to initiate the process of optical damage, either by enhancing the local field strength in regions near the cracks or by providing a source of nearly free electrons needed to initiate the avalanche breakdown process. It is also observed (Lowdermilk and Milam, 1981) that surface damage occurs with a lower threshold at the exiting surface than at the entering surface of an optical material. One mechanism leading to this behavior results from the nature of the electromagnetic boundary conditions at a dielectric/air interface, which lead to a deenhancement in field strength at the entering surface and an enhancement at the exiting surface. This process is illustrated pictorially in Fig. 12.1.1. Another physical mechanism that leads to the same sort of front/back asymmetry is diffraction from defects at the front surface which can lead to significant intensity variation (hot spots) at the exiting surface. This effect has been described, for instance, by Genin et al. (2000).

12.2 Avalanche-Breakdown Model

The avalanche-breakdown mechanism is believed to be the dominant damage mechanism for most pulsed lasers. The nature of this mechanism is that a small number N_0 of free electrons initially present within the optical material are accelerated to high energies through their interaction with the laser field. These electrons can then impact-ionize other atoms within the material, thereby producing additional electrons which are subsequently accelerated by the laser field and which eventually produce still more electrons. Some fraction of the energy imparted to each electron will lead to a localized heating of the material, which can eventually lead to damage of the material due to cracking or melting. The small number of free electrons required to initiate the avalanche breakdown mechanism can be created by several processes,

including thermal excitation, quantum mechanical tunneling by means of the Keldysh mechanism (Ammosov et al., 1986), multiphoton excitation, or free electrons resulting from crystal defects.

We next describe the avalanche-breakdown model in a more quantitative manner. We note that the energy Q imparted to an electron initially at rest and subjected to an electric field $\tilde{E}$ (assumed quasistatic for present) for a time duration t is given by

$$Q = e\tilde{E}d \quad \text{where} \quad d = \tfrac{1}{2}at^2 = \tfrac{1}{2}\left(e\tilde{E}/m\right)t^2 \tag{12.2.1}$$

or

$$Q = e^2\tilde{E}^2t^2/2m \quad \text{for} \quad t \lesssim \tau. \tag{12.2.2}$$

This result holds for times $t \lesssim \tau$, where τ is the mean time between collisions. For longer time durations, the total energy imparted to the electron will be given approximately by the energy imparted to the electron in time interval τ (that is, by $e^2\tilde{E}^2\tau^2/2m$) multiplied by the number of such time intervals (that is, by t/τ), giving

$$Q = e^2\tilde{E}^2t\tau/2m \quad \text{for} \quad t > \tau. \tag{12.2.3}$$

The rate at which the electron gains energy is given in this limit by*

$$P = \frac{dQ}{dt} = e^2\tilde{E}^2\tau/2m. \tag{12.2.4}$$

We next assume that the number density of free electrons $N(t)$ changes in time according to

$$\frac{dN}{dt} = \frac{fNP}{W}, \tag{12.2.5}$$

where W is the ionization threshold of the material under consideration, P is the absorbed power given by Eq. (12.2.4), and f is the fraction of the absorbed power that leads to further ionization so that $1 - f$ represents the fraction that leads to heating. The solution to Eq. (12.2.5) is thus

$$N(t) = N_0e^{gt} \quad \text{where} \quad g = \frac{fe^2\tilde{E}^2\tau}{2Wm}. \tag{12.2.6}$$

---

* This result can also be deduced by noting that the rate of Joule heating of a conducting material is given by

$$NP = \tfrac{1}{2}\sigma\tilde{E}^2,$$

where N is the number density of electrons and σ is the electrical conductivity, which, according to the standard Drude formula, is given by

$$\sigma = \frac{(Ne^2/m)\tau}{1 + \omega^2\tau^2}.$$

This result constitutes a generalization of that of Eq. (12.2.4) and reduces to it in the limit $\omega\tau \ll 1$.

We next introduce the assumption that optical damage will occur if the electron density $N(T_p)$ at the end of the laser pulse of duration T_p exceeds some damage threshold value N_{th}, which is often assumed to be of the order of 10^{18} cm^{-3}. The condition for the occurrence of laser damage can thus be expressed as

$$\frac{fe^2\tilde{E}^2\tau T_p}{2mW} > \ln(N_{\text{th}}/N_0). \tag{12.2.7}$$

The right-hand side of this equality depends only weakly on the assumed values of N_{th} and N_0 and can be taken to have a value of the order of 30. This result can be used to find that the threshold intensity for producing laser damage is given by

$$I_{\text{th}} = n\epsilon_0 c\langle\tilde{E}^2\rangle = 2n\epsilon_0 c\frac{Wm}{fe^2\tau T_p}\ln(N_{\text{th}}/N_0). \tag{12.2.8}$$

If we evaluate this expression under the assumption that $n \approx 1$, $W \approx 5$ eV, $\tau \approx 10^{-15}$ s, $T_p \approx 10^{-9}$ s, and $f \approx 0.01$, we find that $I_{\text{th}} \simeq 40$ GW/cm^2, in reasonable agreement with measured values.

12.3 Influence of Laser Pulse Duration

There is a well-established scaling law that relates the laser damage threshold to the laser pulse duration T_p for pulse durations in the approximate range of 10 ps to 10 ns. In particular, this scaling law states that the fluence (energy per unit area) required to produce damage increases with pulse duration as $T_p^{1/2}$, and correspondingly the intensity required to produce laser damage decreases with pulse duration as $T_p^{-1/2}$. This scaling law can be interpreted as a statement that (for this range of pulse durations) optical damage depends not solely on laser fluence or on laser intensity but rather upon their geometrical mean. It should be noted that this observed scaling law is inconsistent with the predictions given by the simple model that leads to Eq. (12.2.8), which implies that laser damage should depend only on the laser intensity. Some possible physical processes that could account for this discrepancy are described below. Data illustrating the observed scaling law are shown in Fig. 12.3.1, and more information regarding this law can be found in Lowdermilk and Milam (1981) and Du et al. (1994).

The $T_p^{1/2}$ scaling law can be understood, at least in general terms, by noting that the avalanche-breakdown model ascribes the actual damage mechanism to rapid localized heating of the optical material. The local temperature distribution $T(\mathbf{r}, t)$ obeys the heat transport equation (see also Eq. (4.5.2))

$$(\rho C)\frac{\partial\tilde{T}}{\partial t} - \kappa\nabla^2\tilde{T} = N(1-f)\tilde{P}, \tag{12.3.1}$$

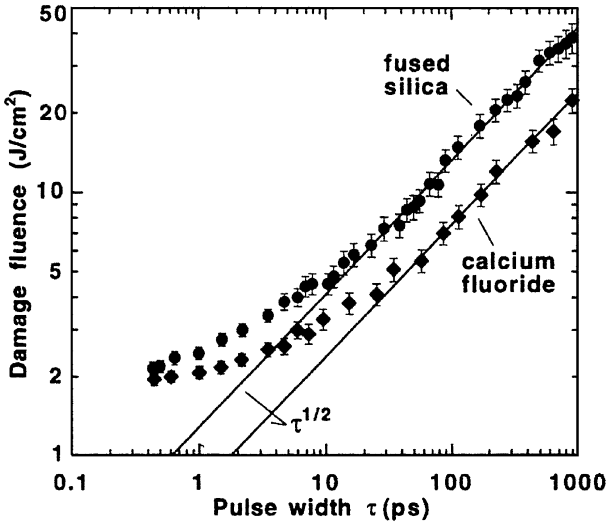

FIGURE 12.3.1: Measured dependence of laser damage threshold on laser pulse duration (Stuart et al., 1995).

where f, N, and P have the same meanings as in the previous section, κ is the thermal conductivity, and (ρC) is the heat capacity per unit volume. Let us temporarily ignore the source term on the right-hand side of this equation, and estimate the distance L over which a temperature rise ΔT will diffuse in a time interval T_p. Replacing derivatives with ratios and assuming diffusion in only one dimension, as indicated symbolically in Fig. 12.3.2, we find that

$$(\rho C)\frac{\Delta T}{T_p} = \kappa \frac{\Delta T}{L^2}, \tag{12.3.2}$$

or that

$$L = (DT_p)^{1/2} \quad \text{where} \quad D = \kappa/\rho c \text{ is the diffusion constant.} \tag{12.3.3}$$

The heat deposited by the laser pulse is thus spread out over a region of dimension L that is proportional to $T_p^{1/2}$, and the threshold for optical damage will be raised by this same factor. Although this explanation for the $T_p^{1/2}$ dependence is widely quoted, and although it leads to the observed dependence on the pulse duration T_p, some doubt has been expressed (Bloembergen, 1997) regarding whether values of D for typical materials are sufficiently large for thermal diffusion to be important. Nonetheless, detailed numerical calculations (Stuart et al., 1995, 1996) that include the effects of multiphoton ionization, Joule heating, and avalanche ionization are in good agreement with experimental results.

Different considerations come into play for excitation with laser pulses of fsec duration, because under these circumstances the pulse is shorter than some of the material relaxation

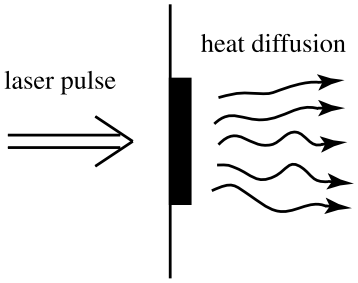

FIGURE 12.3.2: Illustration of the diffusion of heat following absorption of an intense laser pulse.

times. The topic of optical damage from fsec pulses has been treated by Davis et al. (1996), Glezer et al. (1996), and Pronko et al. (1995).

12.4 Direct Photoionization

In this process the laser field strength is large enough to rip electrons away from the atomic nucleus. This process is expected to become dominant if the peak laser field strength exceeds the atomic field strength $E_{\text{at}} = e/4\pi\epsilon_0 a_0^2 = 5 \times 10^{11}$ V/m. Fields this large are obtained at intensities of

$$I_{\text{at}} = \tfrac{1}{2} n \epsilon_0 c E_{\text{at}}^2 \approx 4 \times 10^{16} \text{ W/cm}^2 = 4 \times 10^{20} \text{ W/m}^2.$$

For laser pulses of duration 100 fsec or longer, laser damage can occur at much lower intensities by means of the other processes described above. Direct photoionization is described in more detail in Chapter 13.

12.5 Multiphoton Absorption and Multiphoton Ionization

In this section we calculate the rate at which multiphoton absorption processes occur. Some examples of multiphoton absorption processes are shown schematically in Fig. 12.5.1. Two-photon absorption was first reported experimentally by Kaiser and Garrett (1961).

Some of the reasons for current interest in the field of multiphoton absorption include the following:

1. Multiphoton spectroscopy can be used to study high-lying electronic states and states not accessible from the ground state because of selection rules.
2. Two-photon microscopy (Denk et al., 1990 and Xu and Webb, 1997) has been used to eliminate much of the background associated with imaging through highly scattering materials, both because most materials scatter less strongly at longer wavelengths and because two-

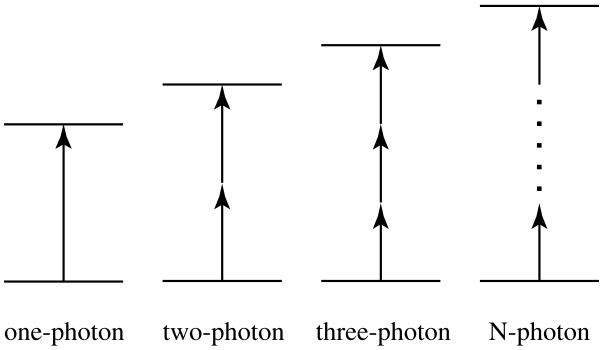

FIGURE 12.5.1: Several examples of multiphoton absorption processes.

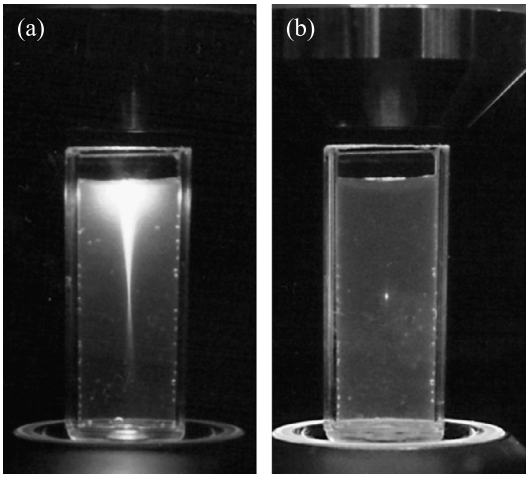

FIGURE 12.5.2: Fluorescence from a dye solution (20 μM solution of fluorescence in water) under (a) one-photon excitation and (b) two-photon excitation. Note that under two-photon excitation, fluorescence is excited only at the focal spot of the incident laser beam. Photographs courtesy of W. Webb.

photon excitation provides sensitivity only in the focal volume of the incident laser beam. Such behavior is shown in Fig. 12.5.2.

3. Multiphoton absorption and multiphoton ionization can lead to laser damage of optical materials and be used to write permanent refractive index structures into the interior of optical materials. See for instance the articles listed at the end of this chapter under the heading Optical Damage with Femtosecond Laser Pulses.
4. Multiphoton absorption constitutes a nonlinear loss mechanism that can limit the efficiency of nonlinear optical devices such as optical switches (see also the discussion in Section 7.3).

In principle, we already know how to calculate multiphoton absorption rates by means of the formulas presented earlier in Chapter 3. For instance, the linear absorption rate is proportional to $\mathrm{Im}\,\chi^{(1)}(\omega)$. Similarly, the two-photon absorption rate is proportional to $\mathrm{Im}\,\chi^{(3)}(\omega = \omega + \omega - \omega)$. We have already seen how to calculate these quantities. However, the method we used to calculate $\chi^{(3)}$ becomes tedious to apply to higher-order processes (e.g., $\chi^{(5)}$ for three-photon absorption, etc.). For this reason, we now develop a simpler approach that generalizes more easily to N-photon absorption for arbitrary N.

12.5.1 Theory of Single- and Multiphoton Absorption and Fermi's Golden Rule

Let us next see how to use the laws of quantum mechanics to calculate single- and multiphoton absorption rates. We begin by deriving the standard result for the single-photon absorption rate, and we then generalize this result to higher-order processes.

The calculation uses procedures similar to those used in Section 3.2 to calculate the nonlinear optical susceptibility. We assume that the atomic wavefunction $\psi(\mathbf{r}, t)$ obeys the time-dependent Schrödinger equation

$$i\hbar\frac{\partial\psi(\mathbf{r}, t)}{\partial t} = \hat{H}\psi(\mathbf{r}, t), \tag{12.5.1}$$

where the Hamiltonian $\hat{H}$ is represented as

$$\hat{H} = \hat{H}_0 + \hat{V}(t). \tag{12.5.2}$$

Here $\hat{H}_0$ is the Hamiltonian for a free atom and

$$\hat{V}(t) = -\hat{\mu}\tilde{E}(t), \tag{12.5.3}$$

where $\hat{\mu} = -e\hat{r}$, is the interaction energy with the applied optical field. For simplicity we take this field as a monochromatic wave of the form

$$\tilde{E}(t) = Ee^{-i\omega t} + \text{c.c.} \tag{12.5.4}$$

that is switched on suddenly at time $t = 0$.

We assume that the solutions to Schrödinger's equation for a free atom are known, and that the wavefunctions associated with the energy eigenstates can be represented as

$$\psi_n(\mathbf{r}, t) = u_n(\mathbf{r})e^{-i\omega_n t}, \quad \text{where} \quad \omega_n = E_n/\hbar. \tag{12.5.5}$$

We see that expression (12.5.5) will satisfy Eq. (12.5.1) (with $\hat{H}$ set equal to $\hat{H}_0$) if $u_n(\mathbf{r})$ satisfies the eigenvalue equation

$$\hat{H}_0 u_n(\mathbf{r}) = E_n u_n(\mathbf{r}). \tag{12.5.6}$$

We return now to the general problem of solving Schrödinger's equation in the presence of a time-dependent interaction potential $\hat{V}(t)$:

$$i\hbar\frac{\partial\psi(\mathbf{r},t)}{\partial t} = \big(\hat{H}_0 + \hat{V}(t)\big)\psi(\mathbf{r},t). \tag{12.5.7}$$

Since the energy eigenstates of $\hat{H}_0$ form a complete set, we can express the solution to Eq. (12.5.7) as a linear combination of these eigenstates—that is, as

$$\psi(\mathbf{r},t) = \sum_l a_l(t)u_l(\mathbf{r})e^{-i\omega_l t}. \tag{12.5.8}$$

We introduce Eq. (12.5.8) into Eq. (12.5.7) and find that

$$\begin{aligned} i\hbar\sum_l \frac{da_l}{dt}u_l(\mathbf{r})e^{-i\omega_l t} + i\hbar\sum_l(-i\omega_l)a_l(t)u_l(\mathbf{r})e^{-i\omega_l t} \\ = \sum_l a_l(t)E_l u_l(\mathbf{r})e^{-i\omega_l t} + \sum_l a_l(t)\hat{V}u_l(\mathbf{r})e^{-i\omega_l t}, \end{aligned} \tag{12.5.9}$$

where (since $E_l = \hbar\omega_l$) clearly the second and third terms cancel. To simplify this expression further, we multiply both sides (from the left) by $u_m^*(\mathbf{r})$ and integrate over all space. Making use of the orthonormality condition

$$\int u_m^*(r)u_l(r)\,d^3r = \delta_{ml}, \tag{12.5.10}$$

we obtain

$$i\hbar\frac{da_m}{dt} = \sum_l a_l(t)V_{ml}e^{-i\omega_{lm}t}, \tag{12.5.11}$$

where $\omega_{lm} = \omega_l - \omega_m$ and where

$$V_{ml} = \int u_m^*(\mathbf{r})\hat{V}u_l(\mathbf{r})\,d^3r \tag{12.5.12}$$

are the matrix elements of the interaction Hamiltonian $\hat{V}$. Eq. (12.5.11) is a matrix form of the Schrödinger equation.

Oftentimes, as in the case at hand, Eq. (12.5.11) cannot be solved exactly and must be solved using perturbation techniques. To this end, we introduce a strength parameter λ which is assumed to vary continuously between zero and one; the value $\lambda = 1$ is taken to correspond to the physical situation at hand. We replace V_{ml} by λV_{ml} in Eq. (12.5.11) and expand $a_m(t)$ in powers of the interaction as

$$a_m(t) = a_m^{(0)}(t) + \lambda a_m^{(1)}(t) + \lambda^2 a_m^{(2)}(t) + \cdots. \tag{12.5.13}$$

By equating powers of λ on each side of the resulting form of Eq. (12.5.11) we obtain the set of equations

$$\frac{da_m^{(N)}}{dt} = (i\hbar)^{-1} \sum_l a_l^{(N-1)} V_{ml} e^{-i\omega_{lm}t}, \quad N = 1, 2, 3, \ldots. \tag{12.5.14}$$

12.5.2 Linear (One-Photon) Absorption

Let us first see how to use Eq. (12.5.14) to describe linear absorption. We set $N = 1$ to correspond to an interaction first-order in the field. We also assume that in the absence of the applied laser field the atom is in the state g (typically the ground state) so that

$$a_g^{(0)}(t) = 1, \qquad a_l^{(0)}(t) = 0 \quad \text{for} \quad l \neq g \tag{12.5.15}$$

for all times t. Through use of Eqs. (12.5.3) and (12.5.4), we represent V_{mg} as

$$V_{mg} = -\mu_{mg}\left(Ee^{-i\omega t} + E^* e^{i\omega t}\right). \tag{12.5.16}$$

Eq. (12.5.14) then becomes

$$\frac{da_m^{(1)}}{dt} = -(i\hbar)^{-1}\mu_{mg}\left[Ee^{i(\omega_{mg}-\omega)t} + E^* e^{i(\omega_{mg}+\omega)t}\right].$$

This equation can be integrated to give

$$\begin{aligned} a_m^{(1)}(t) &= -(i\hbar)^{-1}\mu_{mg}\int_0^t dt'\left[Ee^{i(\omega_{mg}-\omega)t'} + E^* e^{i(\omega_{mg}+\omega)t'}\right] \\ &= \frac{\mu_{mg}E}{\hbar(\omega_{mg}-\omega)}\left[e^{i(\omega_{mg}-\omega)t} - 1\right] + \frac{\mu_{mg}E^*}{\hbar(\omega_{mg}+\omega)}\left[e^{i(\omega_{mg}+\omega)t} - 1\right]. \end{aligned} \tag{12.5.17}$$

The resonance structure of this expression is illustrated schematically in Fig. 12.5.3. Note that the first term in this expression can become resonant for the process of one-photon absorption, and that (if state m lies below state g) the second term can become resonant for the process of stimulated emission. As our present interest is in the process of one-photon absorption, we drop the second term from consideration. The neglect of the second term is known as the rotating wave approximation. Since $a_m^{(1)}(t)$ is a probability amplitude, the probability $p_m^{(1)}(t)$ that the atom is in state m at time t is given by

$$\begin{aligned} p_m^{(1)}(t) &= \left|a_m^{(1)}(t)\right|^2 = \frac{|\mu_{mg}E|^2}{\hbar^2}\left|\frac{e^{i(\omega_{mg}-\omega)t} - 1}{\omega_{mg}-\omega}\right|^2 \\ &= \frac{|\mu_{mg}E|^2}{\hbar^2}\frac{4\sin^2[(\omega_{mg}-\omega)t/2]}{(\omega_{mg}-\omega)^2} \equiv \frac{|\mu_{mg}E|^2}{\hbar^2} f(t), \end{aligned} \tag{12.5.18}$$

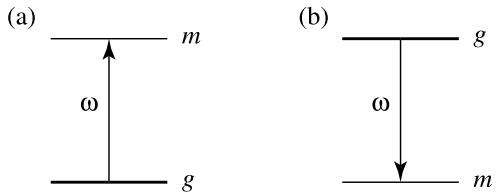

FIGURE 12.5.3: (a) The first term in Eq. (12.5.17) describes the process of one-photon absorption, whereas (b) the second term describes the process of stimulated emission.

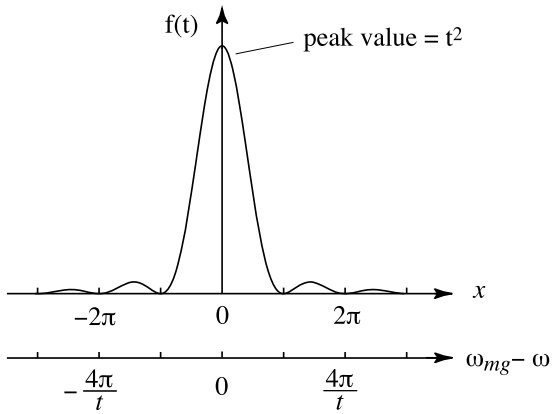

FIGURE 12.5.4: Approximation of $f(t)$ of Eq. (12.5.20) as a Dirac delta function.

where

$$f(t) = \frac{4\sin^2[(\omega_{mg} - \omega)t/2]}{(\omega_{mg} - \omega)^2}. \tag{12.5.19}$$

Let us examine the time dependence of this expression for large values of the interaction time t. Note that we can express $f(t)$ as

$$f(t) = t^2\left(\frac{\sin^2 x}{x^2}\right) \quad \text{where} \quad x \equiv (\omega_{mg} - \omega)t/2. \tag{12.5.20}$$

Note further (see also Fig. 12.5.4) that the peak value of $f(t)$ is t^2, but the width of the central peak is of the order of $2\pi/t$. Thus, the area under the central peak is of the order of $2\pi t$, and for large t the function becomes highly peaked. These facts suggest that, for large t, $f(t)$ is proportional to t times a Dirac delta function. In fact, it can be shown that

$$\lim_{t\to\infty} f(t) = 2\pi t\delta(\omega_{mg} - \omega). \tag{12.5.21}$$

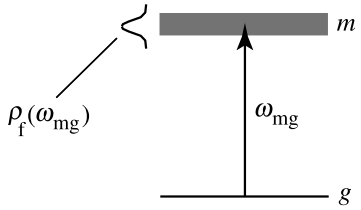

FIGURE 12.5.5: Level m is spread into a density of states described by the function $\rho_f(\omega_{mg})$.

Thus, for large t the probability to be in the upper level m can be represented, at least formally, by

$$p_m^{(1)}(t) = \frac{|\mu_{mg}E|^2 t}{\hbar^2} 2\pi\delta(\omega_{mg} - \omega). \tag{12.5.22}$$

This result is somewhat unphysical because of the presence of the delta function on the right-hand side. The origin of this unphysical behavior is our assumption that the transition frequency ω_{mg} is taken to be perfectly well defined. In fact, in physically realistic situations, the transition frequency ω_{mg} is not perfectly well defined but is spread into a continuous distribution by various line-broadening mechanisms, as illustrated schematically in Fig. 12.5.5. One often expresses this thought by saying that the final state m is spread into a density of final states $\rho_f(\omega_{mg})$, defined such that $\rho_f(\omega_{mg})d\omega_{mg}$ is the probability that the transition frequency lies between ω_{mg} and $\omega_{mg} + d\omega_{mg}$. In the context of atomic physics, $\rho_f(\omega_{mg})$ is often known as the atomic lineshape function. The density of final states is normalized such that

$$\int_0^\infty \rho_f(\omega_{mg})\, d\omega_{mg} = 1. \tag{12.5.23}$$

A well-known example of a density of final states is the Lorentzian lineshape function

$$\rho_f(\omega_{mg}) = \frac{1}{\pi} \frac{\Gamma/2}{(\bar{\omega}_{mg} - \omega_{mg})^2 + (\Gamma/2)^2} \tag{12.5.24}$$

where $\bar{\omega}_{mg}$ is the line-center transition frequency and Γ is the full-width at half maximum of the distribution in angular frequency units. For a transition broadened by the finite lifetime of its upper level, Γ is the population decay rate of the upper level.

For a transition characterized by a density of final states, the probability $p_m^{(1)}(t)$ to be in the upper level given by Eq. (12.5.22) must be averaged over all possible values of the transition frequency. One obtains

$$\begin{aligned} p_m^{(1)}(t) &= \frac{|\mu_{mg}E|^2 t}{\hbar^2} \int_0^\infty \rho_f(\omega_{mg}) 2\pi\delta(\omega_{mg} - \omega)\, d\omega_{mg} \\ &= \frac{2\pi|\mu_{mg}E|^2 t}{\hbar^2} \rho_f(\omega_{mg} = \omega). \end{aligned} \tag{12.5.25}$$

The notation $\rho_f(\omega_{mg} = \omega)$ means that the density of final states is to be evaluated at the frequency ω of the incident laser light. Since the probability for the atom to be in the upper level is seen to increase linearly with time, we can define a transition rate for linear absorption as

$$R_{mg}^{(1)} = \frac{p_m^{(1)}(t)}{t} = \frac{2\pi|\mu_{mg}E|^2}{\hbar^2}\rho_f(\omega_{mg} = \omega). \tag{12.5.26}$$

This result is a special case of what is known as Fermi's golden rule. Linear absorption is often described in terms of an absorption cross section $\sigma_{mg}^{(1)}(\omega)$, defined such that

$$R_{mg}^{(1)} = \sigma_{mg}^{(1)}(\omega)I, \tag{12.5.27}$$

where $I = 2n\epsilon_0 c|E|^2$. By comparison with Eq. (12.5.26) we find that

$$\sigma_{mg}^{(1)}(\omega) = \frac{\pi}{n\epsilon_0 c}\frac{|\mu_{mg}|^2}{\hbar^2}\rho_f(\omega_{mg} = \omega). \tag{12.5.28}$$

12.5.3 Two-Photon Absorption

Let us next treat the case of two-photon absorption. To do so, we need to solve the set of equations (12.5.14) for $N = 1$ and $N = 2$ to obtain the second-order probability amplitude $a_n^{(2)}(t)$ for the atom to be in level n at time t. The conventions for labeling the various levels are shown in Fig. 12.5.6. Our strategy is to solve Eq. (12.5.14) first for $N = 1$ to obtain $a_m^{(1)}(t)$, which is then used on the right-hand side of Eq. (12.5.14) with $N = 2$. In fact, the expression we obtain for $a_m^{(1)}(t)$ is identical to that of Eq. (12.5.17), obtained in our treatment of linear absorption. We again drop the second term (which does not lead to two-photon absorption). In addition, we express V_{nm} as follows:

$$\begin{aligned} V_{nm} &= -\mu_{nm}\left(Ee^{-i\omega t} + E^*e^{i\omega t}\right) \\ &\simeq -\mu_{nm}Ee^{-i\omega t}. \end{aligned} \tag{12.5.29}$$

Here we have dropped the negative-frequency contribution to V_{nm} for reasons analogous to those described above in connection with Eq. (12.5.17). We thus obtain

$$\begin{aligned} \frac{d}{dt}a_n^{(2)}(t) &= (i\hbar)^{-1}\sum_m a_m^{(1)}(t)V_{nm}e^{-i\omega_{mn}t} \\ &= -(i\hbar)^{-1}\sum_m \frac{\mu_{nm}\mu_{mg}E^2}{\hbar(\omega_{mg} - \omega)}\left[e^{i(\omega_{ng}-2\omega)t} - e^{i(\omega_{nm}-\omega)t}\right]. \end{aligned} \tag{12.5.30}$$

We next drop the second term in square brackets, which describes the transient response of the system but does not lead to two-photon absorption. The resulting equation can be integrated

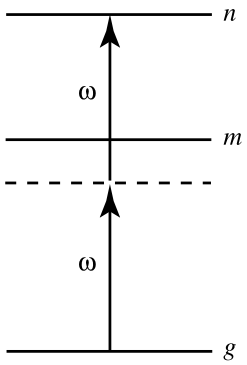

FIGURE 12.5.6: Definition of energy levels used in the calculation of the two-photon transition rate.

directly to obtain

$$a_n^{(2)}(t) = \sum_m \frac{\mu_{nm}\mu_{mg}E^2}{\hbar^2(\omega_{mg}-\omega)}\left[\frac{e^{i(\omega_{mg}-2\omega)t}-1}{\omega_{ng}-2\omega}\right]. \tag{12.5.31}$$

The calculation now proceeds analogously to that for the linear absorption. The probability to be in level n is given by

$$p_n^{(2)}(t) = \left|a_n^{(2)}(t)\right|^2 = \left|\sum_m \frac{\mu_{nm}\mu_{mg}E^2}{\hbar^2(\omega_{mg}-\omega)}\right|^2 \left|\frac{e^{i(\omega_{mg}-2\omega)t}-1}{\omega_{ng}-2\omega}\right|^2. \tag{12.5.32}$$

For large t, the expression becomes (using the same reasoning as in Eqs. (12.5.18)–(12.5.22))

$$p_n^{(2)}(t) = \left|\sum_m \frac{\mu_{nm}\mu_{mg}E^2}{\hbar^2(\omega_{mg}-\omega)}\right|^2 2\pi t\delta(\omega_{ng}-2\omega), \tag{12.5.33}$$

and if we assume that level n is smeared into a density of states we obtain

$$p_n^{(2)}(t) = \left|\sum_m \frac{\mu_{nm}\mu_{mg}E^2}{\hbar^2(\omega_{mg}-\omega)}\right|^2 2\pi t\rho_f(\omega_{ng}=2\omega). \tag{12.5.34}$$

Since the probability for the atom to be in the upper level is seen to increase linearly with time, we can define a transition rate for two-photon absorption given by

$$R_{ng}^{(2)} = \frac{p_n^{(2)}(t)}{t}. \tag{12.5.35}$$

It is convenient to recast this result in terms of a two-photon cross section defined by

$$R_{ng}^{(2)} = \sigma_{ng}^{(2)}(\omega)I^2, \tag{12.5.36}$$

where $I = 2n\epsilon_0 c|E|^2$ is the intensity of the incident light beam. We find that

$$\sigma_{ng}^{(2)}(\omega) = \frac{1}{4n^2\epsilon_0^2 c^2}\left|\sum_m \frac{\mu_{nm}\mu_{mg}}{\hbar^2(\omega_{mg}-\omega)}\right|^2 2\pi\rho_f(\omega_{ng}=2\omega). \tag{12.5.37}$$

Experimentally, two-photon cross sections are often quoted with intensities measured in photons per unit area per unit time. The two-photon cross section thus has dimensions of area-squared times time per photon, with units of $\mathrm{m}^4\,\mathrm{s\,photon}^{-1}$. Cross sections are often measured in units of Göppert-Mayer (GM), where 1 GM is equal to $10^{-58}\ \mathrm{m}^4\,\mathrm{s\,photon}^{-1}$ or $10^{-50}\ \mathrm{cm}^4\,\mathrm{s\,photon}^{-1}$. With this convention, Eqs. (12.5.36) and (12.5.37) must be replaced by

$$R_{ng}^{(2)} = \bar{\sigma}_{ng}^{(2)}(\omega)\bar{I}^2 \quad \text{where} \quad \bar{I} = \frac{2n\epsilon_0 c}{\hbar\omega}|E|^2 \tag{12.5.38}$$

and where

$$\bar{\sigma}_{ng}^{(2)}(\omega) = \frac{\omega^2}{4n^2\epsilon_0^2 c^2}\left|\sum_m \frac{\mu_{nm}\mu_{mg}}{\hbar(\omega_{mg}-\omega)}\right|^2 2\pi\rho_f(\omega_{ng}=2\omega). \tag{12.5.39}$$

We can perform a numerical estimate of $\bar{\sigma}^{(2)}$ by assuming that a single level dominates the sum in Eq. (12.5.39) and assuming that the one-photon transition is highly nonresonant so that $\omega_{mg} - \omega \approx \omega$. We also assume that the laser frequency is tuned to the peak of the two photon resonance, so that $\rho_f(\omega_{ng}=2\omega) \approx (2\pi\Gamma_n)^{-1}$, where Γ_n is the width of level n. We then obtain

$$\bar{\sigma}_{ng}^{(2)} \approx \frac{|\mu_{nm}\mu_{mg}|^2}{4\epsilon_0^2\hbar^2 c^2\Gamma_n}. \tag{12.5.40}$$

To evaluate this expression, we assume that both μ_{nm} and μ_{mg} are of the order of $ea_0 = 8 \times 10^{-30}$ Cm and that $\Gamma_n = 2\pi(1 \times 10^{13})$ rad/sec. We then obtain

$$\bar{\sigma}_{ng}^{(2)} \approx 2.5 \times 10^{-58}\frac{\mathrm{m}^4\ \mathrm{s}}{\mathrm{photon}^2}. \tag{12.5.41}$$

This value is in good order-of-magnitude agreement with those measured by Xu and Webb (1996) for a variety of molecular fluorophores. There can be considerable variation in the values of molecular two-photon cross sections. Drobizhev et al. (2001) report a two-photon cross section as large as $1.1 \times 10^{-54}\ \mathrm{m}^4\ \mathrm{sec/photon}^2$ in a dendrimer molecule.

12.5.4 Multiphoton Absorption

The results of this section are readily generalized to higher-order processes. One obtains, for instance, the following set of relations:

$$R_{mg}^{(1)} = \left| \frac{\mu_{mg} E}{\hbar} \right|^2 2\pi \rho_f(\omega_{mg} - \omega), \tag{12.5.42}$$

$$R_{ng}^{(2)} = \left| \sum_m \frac{\mu_{nm}\mu_{mg} E^2}{\hbar^2(\omega_{mg} - \omega)} \right|^2 2\pi \rho_f(\omega_{ng} - 2\omega), \tag{12.5.43}$$

$$R_{og}^{(3)} = \left| \sum_{mn} \frac{\mu_{on}\mu_{nm}\mu_{mg} E^3}{\hbar^3(\omega_{ng} - 2\omega)(\omega_{mg} - \omega)} \right|^2 2\pi \rho_f(\omega_{og} - 3\omega), \tag{12.5.44}$$

$$R_{pg}^{(4)} = \left| \sum_{omn} \frac{\mu_{po}\mu_{on}\mu_{nm}\mu_{mg} E^4}{\hbar^4(\omega_{og} - 3\omega)(\omega_{ng} - 2\omega)(\omega_{mg} - \omega)} \right|^2 2\pi \rho_f(\omega_{pg} - 4\omega), \tag{12.5.45}$$

and so on.

Problems

1. *Relation between the two-photon absorption cross section and* $\chi^{(3)}$. Derive an expression relating the two-photon absorption cross section $\sigma^{(2)}$ to the third-order susceptibility $\chi^{(3)}$. Be sure to indicate the frequency dependence of $\chi^{(3)}$.
2. *Multiphoton absorption coefficients.* Starting with the expressions for the rates of one-, two-, and three-photon absorption quoted above, deduce expressions for the one-, two-, and three-photon absorption coefficients α, β, and γ defined by the equation

$$\frac{dI}{dz} = -\alpha I - \beta I^2 - \gamma I^3.$$

   Make order-of-magnitude estimates of β and γ for condensed matter, and compare them to typical measured values as tabulated in the scientific literature.

References

Optical Damage

Ammosov, M.V., Delone, N.B., Krainov, V.P., 1986. Sov. Phys. JETP 64, 1191.
Bloembergen, N., 1997. J. Nonlinear Opt. Phys. Mater. 6, 377.
Du, D., Liu, X., Korn, G., Squier, J., Mourou, G., 1994. Appl. Phys. Lett. 64, 3071.
Genin, F.Y., Feit, M.D., Kozlowski, M.R., Rubenchik, A.M., Salleo, A., Yoshiyama, J., 2000. Appl. Opt. 39, 3654.
Stuart, B.C., Feit, M.D., Rubenchik, A.M., Shore, B.W., Perry, M.D., 1995. Phys. Rev. Lett. 74, 2248.
Stuart, B.C., Feit, M.D., Herman, S., Rubenchik, A.M., Shore, B.W., Perry, M.D., 1996. Phys. Rev. B 53, 1749.

Reviews of Optical Damage

Bloembergen, N., 1974. IEEE J. Quantum Electron. 10, 375.
Lowdermilk, W.H., Milam, D., 1981. IEEE J. Quantum Electron. 17, 1888.
Manenkov, A.A., Prokhorov, A.M., 1986. Sov. Phys. Usp. 29, 104.
Raizer, Y.P., 1965. Sov. Phys. JETP 21, 1009.
Wood, R.M., 1986. Laser Damage in Optical Materials. Adam Hilger, Bristol.

Optical Damage with Femtosecond Laser Pulses

Davis, K.M., Miura, K., Sugimoto, N., Hirao, K., 1996. Opt. Lett. 21, 1729.
Glezer, E.N., Milosavljevic, M., Huang, L., Finlay, R.J., Her, T.-H., Callan, J.P., Mazur, E., 1996. Opt. Lett. 21, 2023.
Pronko, P.P., Dutta, S.K., Squier, J., Rudd, J.V., Du, D., Mourou, G., 1995. Opt. Commun. 114, 106.

Multiphoton Absorption

Denk, W., Strickler, J.H., Webb, W.W., 1990. Science 248, 73.
Drobizhev, M., Karotki, A., Rebane, A., Spangler, C.W., 2001. Opt. Lett. 26, 1081.
Kaiser, W., Garrett, C.G.B., 1961. Phys. Rev. Lett. 7, 229.
Xu, C., Webb, W.W., 1996. J. Opt. Soc. Am. B 13, 481.
Xu, C., Webb, W.W., 1997. In: Lakowicz, J. (Ed.), Topics in Fluorescence Spectroscopy, vol. 5: Nonlinear and Two-Photon-Induced Fluorescence. Plenum Press, New York, Chapter 11.